

LASER-PROBING THE NANOCOSMOS*

E. Vandeweert¹, V. Philippsen^{1,+}, J. Bastiaansen¹, F. Vervaecke¹, P. Lievens¹
R.E. Silverans¹, P Cyganik², Z Postawa², C.A Meserole³ and N. Winograd³

¹ *Laboratorium voor Vaste-Stoffysica en Magnetisme, Katholieke Universiteit
Leuven, Celestijnenlaan 200D, B-3001 Leuven*

⁺ *presently at IMEC, Kapeldreef 75, B-3001 Leuven*

² *Institute of Physics, Jagellonian University, ul. Reymonta 4, PL 30-059 Krakow,
Poland*

³ *Department of Chemistry, The Pennsylvania State University, University Park, PA
16802, USA*

* Summary of the work, awarded with the prize of the best oral presentation by E. Vandeweert at the General Scientific Meeting of the Belgian Physical Society, Leuven, May 16-17, 2001

In this review we demonstrate how laser photo-ionization in combination with mass spectrometry is a versatile and extremely sensitive technique to study particle – solid interactions. The combined interpretation of the observables accessible with this technique, including population partitions, (quantum-state selective) velocity and angular distributions, and molecular fragmentation patterns, allows for gaining valuable insight in particle-induced desorption processes. These processes were found to depend strongly on the physical and chemical nature of the systems under study. We present results from three case studies of systems with increasing chemical complexity subjected to keV Ar⁺ ion bombardment. In the first case, the importance of resonant electron transfer in governing the final electronic configuration of metastable atoms emitted from clean metallic surfaces is introduced. Next, we focus on the mechanisms that govern the lift-off of intact molecules from ion-bombarded silver surfaces covered with a thin layer of physisorbed frozen benzene. Finally, we discuss how both ballistic processes as well as chemical reactions lead to the desorption of molecular fragments from highly ordered self-assembled monolayers covalently bound to a gold substrate.

1. Introduction

Surface characterization techniques are becoming increasingly sophisticated and sensitive to keep up with the constant reduction of the amount of material available for the analysis. Many nanotechnological applications presently under development rely, for example, on functionalized surfaces with only a submonolayer coverage of complex organic molecules [1]. Laser photo-ionization in combination with mass

spectrometry is a unique and valuable technique for the state-, energy- and angle-resolved detection of neutral atoms and molecules in the gas phase with unmatched sensitivity. We demonstrate how laser probing can be exploited to study in-situ the processes that occur during the dynamical interaction of surfaces with energetic projectiles. A better understanding of these processes not only is essential from a fundamental physics point-of-view, but also has technological implications. The study of the effects related to the exposure of organic surfaces to swift charged particles is thereby of special interest. This is important for applications such as the development of ultra thin lithographic resists or the use of devices based on functionalized surfaces in hostile environments. It also allows for the evaluation of the radiation-induced damage during characterization sessions by standard spectroscopic techniques. Up to now, most studies focused on the interpretation of the structural changes in pristine systems after irradiation. Little information is available on the dynamical behavior of the films during the interaction with the projectiles, and even less is known on the particle-initiated desorption processes.

Recently quite some experimental effort is being put in unraveling the processes that occur during the emission of neutral species upon impact of energetic projectiles on pure metallic substrates and on substrates covered with thin organic overlayers. When an ion with a kinetic energy of a few keV hits a metallic surface, atoms, clusters and molecules are released in different electronic and charge states. This is commonly known as sputtering. The main kinematic aspects of such a sputter event, like the overall yield or the energy and angular distributions, are reasonably well described by cascade theory based on the transfer of collisional energy and momentum [2]. But the underlying physics and chemistry that govern, e.g., the final internal energy an ejected particle ends up with, can be quite different depending on the specific system under investigation, and are largely not understood [3-5].

In this paper we give a review of experimental results that were obtained from three systems with an increasing chemical complexity. We first describe the contribution of electronic processes during the ejection of an atomic particle upon impact of an energetic ion on a clean metallic surface. Next, we focus on the mechanisms that govern the lift-off of intact molecules from ion-bombarded silver surface covered with a thin layer of frozen benzene. Finally, the processes that occur during the ion-stimulated erosion of self-assembled monolayers deposited on gold are discussed. As all results are obtained using (resonance) laser photo-ionization as experimental

technique, we start with a condensed summary of the setups and employed procedures.

2. Experimental setup

The measurements presented in this paper were performed in two different laser-ionization mass spectrometers. Such an experimental setup basically consists of three main parts: an ion gun used to release particles from solid samples into the gas phase, the ionizing-laser system(s) and a mass filter with a charge-sensitive detector. To reduce the rate of surface contamination as much as possible, the samples are positioned in an ultrahigh vacuum environment (base pressure of at least 5×10^{-10} hPa) and – in case of bulk metallic samples – thoroughly cleaned by prolonged continuous ion bombardment before the experiment.

Full details of the Leuven resonance ionization mass spectrometer can be found elsewhere [6,7]. Briefly, clean metallic samples are bombarded by 15 keV Ar^+ ions directed at 45° incidence onto the target. The ion gun can be operated in a continuous (with current densities of ca. $0.5 \mu\text{A}/\text{cm}^2$) or pulsed mode (pulse duration ca. 300 ns). Linearly polarized light is generated by two independent laser systems: an optical parametric oscillator (tuning range 225-1600 nm) and a dye laser both pumped by pulsed Nd:YAG lasers. Both laser systems are equipped with frequency doubling units. The laser pulse duration is about 6 ns and the pulses have a bandwidth of ca. 10 GHz. Maximum pulse energies range from a few mJ in the UV up to 50 mJ in the visible wavelength region. The laser beams intersect the sputtered plume perpendicularly to the axis of ion extraction and 4 mm in front of the sample surface. The laser-ionized particles are finally extracted into a reflectron-type time-of-flight mass spectrometer (with a typical mass resolution of about 800 at 60 a.m.u.) and detected using standard dual microchannel plates.

The experimental setup at Penn State is designed to measure energy- and angular-resolved distributions of neutral (EARN) particles and has been described in detail elsewhere [8]. Desorption events are initiated by a 200 ns 8 keV Ar^+ ion pulse focused to a spot with a diameter of 3 mm on the sample surface. The measurements were performed under static conditions with the accumulated primary ion dose kept at 10^{11} ions/ cm^2 to limit the accumulation of surface damage as much as possible. The plume of desorbed particles is intersected about 10 mm in front of the sample by either one or two ribbon-shaped laser beams from pulsed Nd:YAG pumped dye laser

systems. Typical output energies are of the order of 1 mJ in 6ns pulses, while the bandwidth is of the order of 10 GHz. Desorbed particles are subsequently mass-selectively detected using a gated, position-sensitive microchannel plate detector.

3. Experimental procedures

Basically, four experimental observables are accessible using these setups: (i) mass spectra (ii) population partitions (iii) (state-selective) flight-time distributions and (iv) (state-selective) angular distributions.

Recording mass spectra not only introduces Z-selectivity when performing measurements on atoms of elements with multiple isotopes (which in general cannot be resolved spectrally due to the large bandwidth of employed laser systems), but also allows discrimination against non-resonantly ionized species. The photo-ionization of more complex aggregates such as clusters and molecules is almost always accompanied with some degree of photofragmentation. Moreover, the impact of an energetic particle on a molecular overlayer results in the desorption of molecular fragments. Fragmentation patterns compiled from the mass spectra contain valuable information to disentangle the fragmentation processes involved.

Gas-phase atoms and molecules are distributed over different discrete levels according to their internal energy. If the energy difference between the levels is larger than the laser bandwidth and the lifetime of the excited particles is long enough to detect them a few μs after they are created, state-selective photo-ionization allows for comparing the populations on different levels. Recently, a number of new experiments were performed based on the state-selective detection of free atoms and small molecules by resonance laser ionization spectroscopy. This technique proves to be unique and universally applicable for the quantitative determination of population partitions of atoms sputtered in the ground and metastable electronic states and even small molecules in ground and vibrationally excited states [4,7,9].

To quantitatively determine the population partition of sputtered atoms an experimental procedure based on two-step two-color resonance laser ionization was used. The first step sequentially saturates the excitation of atoms in different envisaged states into a selected intermediate state. A second and independent ionization step is used to ionize the atoms. Where possible, the same intermediate state is used to deduce directly the relative population from the relative photo-ion signals, taking into account the degeneracies of the states involved, regardless of the

ionization efficiency: only saturation of the excitation step is needed which is easily obtained at modest laser pulse energies. Due to the extended range of values for the total angular momentum of most atoms, selection rules governing optical transitions prohibit that the populations in all metastable states are probed via a single intermediate state. The overall partition is then obtained by combining population distributions of overlapping subsets of metastable states. A more detailed discussion of this experimental procedure can be found in Refs. [6,7].

The quantum-state selective flight-time distributions of the sputtered atoms and molecules are recorded by varying the delay between the impact of the ion pulse and the firing of the laser pulse(s). Velocity or kinetic energy distributions are then obtained after coordinate transformation of the measured flight-time distributions using the appropriate sample-to-laser distance [7,8,10].

Finally, the position-sensitive detector in the Penn State system enables the calculation of the polar ejection angle distribution of the sputtered particles. This allows for collecting simultaneously energy and angular-resolved data from desorbed neutral atoms and molecules.

4. Resonant electron transfer during sputtering of metals

To date, the electronic processes involved in the determination of the final state *of a particle sputtered from a pure metal* upon keV ion-bombardment are poorly understood. Current popular models include collisional excitation at or above the surface, bond-breaking of quasimolecules, and electron transfer between the metal and the sputtered particles, but fail to give a unified picture [3,4]. Present work in exploring the different electronic processes and their relative importance during the sputter event is focusing on the emission of metastable atoms following the ion-beam sputtering of simple metallic systems. Once the interaction between the escaping particle and the metal is terminated, metastable atoms (with lifetimes of the order of seconds) preserve their excitation state until they are detected at large distances from the surface.

In order to compile a more complete picture of the electronic processes that occur during ion-beam sputtering of metals, we performed measurements on a series of different metals, including Co, Ni, Cu, Sr, Ag, and Ir, that exhibit a rich structure of low- and high-lying metastable states with different electronic configurations. Population partitions and state-selective velocity distributions of ground state and

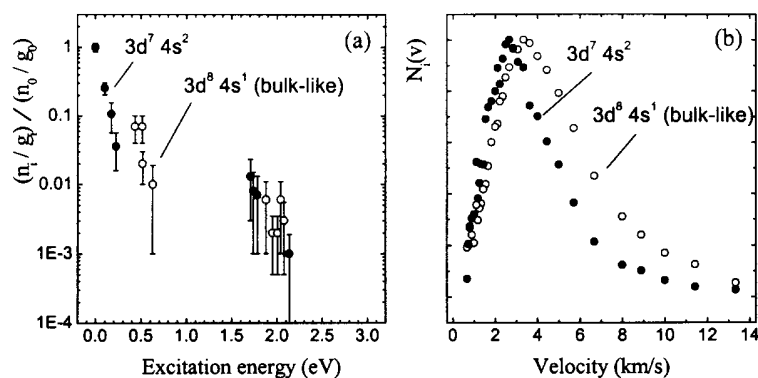


Fig. 1. (a) Population distribution of sputtered Co atoms produced by 15 keV Ar^+ ion bombardment of a pure polycrystalline target. The populations (n_i) are given relative to the ground state and corrected for the statistical weight of each state (g_i). (b) State-selected velocity distributions of Co atoms. Representative examples are given for atoms sputtered in a state with a $3d^8 4s^2$ (closed symbols) and a $3d^9 4s^1$ (open symbols) configuration. This last configuration has the closest resemblance with the bulk electronic structure (“bulk like”).

metastable atoms contain key information on the initial sputter event. An example of such a population partition and two state-selective velocity distributions are shown in Fig. 1a and b resp. The combined interpretation of these observables thus allows us to gain more insight in the electronic mechanisms that occur during the sputtering process. These investigations were strongly indicative that the population of the atomic ground state and metastable states is largely governed by a mechanism sensitive to the electronic configuration of the atomic state [11-13].

For an extensive overview of the results of this parametric study and a discussion of the physical interpretation within the resonant- electron transfer model, we refer to the paper by Dr. Vicky Philipson in this volume of *Physica*.

5. State-selective detection of neutral molecules ejected from keV bombarded $\text{C}_6\text{H}_6/\text{Ag}(111)$

The impact of an energetic ion on a *metallic substrate covered with an organic overlayer* triggers a chain of events that finally leads to the ejection of both substrate atoms and intact adsorbate molecules. Such a desorption process is based on different mechanisms in which the properties of the incident particle, of the metal, and of the molecular overlayer contribute. Recently, experimental evidence in combination with an increased understanding at a microscopic level gained from molecular dynamics simulations allowed different mechanisms that lead to the desorption of molecules from simple, well-defined systems to be discerned [5,14,15]. We used resonant laser

ionization spectroscopy to monitor quantum-state selectively both desorbed neutral molecules and atoms sputtered from the underlying substrate as function of adsorbate coverage.

As a model system we selected benzene physisorbed on the (111) planes of a cold clean silver crystal. This system is chosen because of a number of attractive attributes. Chemical reactions between the silver and the benzene that can modify the simple binary nature of the system can be largely neglected because of the inert nature of silver toward benzene. The system is reversible with temperature and highly reproducible. Moreover, the energy level system for both benzene and silver are well documented and their ultraviolet spectra are experimentally easily accessible.

Before the measurements, the Ag(111) single crystal is cleaned by many cycles of continuous ion bombardment and by annealing at 730 K until a sharp LEED pattern is obtained. Freeze-pump-thaw cycles are performed to remove gaseous impurities from the benzene. Benzene is dosed onto the cold (120 K) Ag crystal by backfilling the chamber, and different coverages were obtained by controlling the pressure and the exposure period. All exposures are reported in Langmuirs (1 Langmuir (L) equals 1×10^{-6} Torr.s). Benzene is known to form ordered (3×3) overlayers on Ag(111) from a 5 L exposure [16], and 5-7 L exposures correspond to approx. 1 monolayer (ML) coverage [17].

The results allow us to compile a detailed picture of the desorption process in this model system. A substantial part of the substrate atoms were detected to be sputtered into a very high-lying metastable state. The yield in this excited state was found to decrease rapidly as the amount of benzene covering the crystal surface increased. Also the kinetic energy and angular distributions were found to be modified upon dosing. The results indicate that a large fraction of the metastable silver atoms de-excite during collisions with the adsorbate molecules [9,17].

Previously, non-resonant laser postionization was used to study the coverage-dependent molecular ejection from ion-bombarded $C_6H_6/Ag(111)$ [14]. The results obtained from kinetic energy and angular distributions and the relative yield of neutral C_6H_6 molecules suggest that depending on the thickness of the overlayer, more than one mechanism is responsible for the ejection process. The experiments presented here allow for differentiation between the behavior of molecules with different internal energies. As such they provide a unique possibility to gain even further

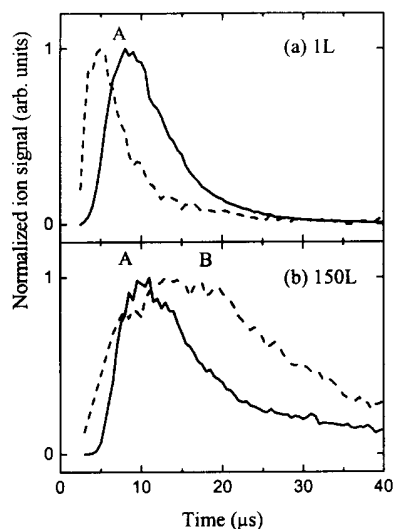


Fig. 2. State selective flight time distributions of neutral benzene molecules desorbed from C_6H_6 on $Ag(111)$ at (a) a submonolayer (1L exposure) and (b) multilayer coverage (150 L exposure). Solid lines represent the distributions obtained for C_6H_6 while the dashed lines show the distributions for $C_6H_6^*$.

the width and the position of the peak depend strongly on the state in which the particle leaves the surface, as well as on the benzene coverage. Not surprisingly, the coverage-dependent desorption of benzene molecules bears great similarity with the results previously obtained by non-resonant ionization of ejected benzene molecules [14]. From these experiments, it was learned that a peak appearing at short flight times (labeled "A" in Fig. 2) was attributed to benzene molecules having a most probable kinetic energy of about 1 eV and desorbed by collisions with substrate particles. As the coverage increases, the number of less energetic intermolecular collisions grows resulting in a broadened flight-time distribution that is peak-shifted towards longer flight times (lower kinetic energies). Finally, upon high exposures a pronounced second feature appears in the time distribution at large flight times (indicated by "B" in Fig. 2). This maximum is composed of benzene molecules that are emitted with a very low most probable kinetic energy of 0.04 eV. At intermediate coverages, such as the one presented here, both peak A and B are discernible, indicating that both desorption mechanisms are competing, while at very high coverages, only peak B is present [14].

insight into the underlying mechanisms responsible for the ejection of large fragile molecules.

Resonant two-photon one-color photoionization of the ejected benzene molecules was achieved by pumping the 6_0^1 transition originating from the zero level of the molecular ground state (C_6H_6), and the 6_1^0 transition starting from the first vibrationally excited state of the ν_6^* mode ($C_6H_6^*$), lying 0.1 eV above the molecular ground state [18].

In Fig. 2, the flight-time density distributions of desorbed C_6H_6 and $C_6H_6^*$ molecules are shown for a 1L exposure (submonolayer coverage) and a 150 L exposure (multilayer coverage). Both

The flight-time distributions of the vibrationally excited $C_6H_6^*$ molecules allow for compiling a more detailed picture on the ejection mechanisms. At low coverages, the time distribution of $C_6H_6^*$ is found to be more narrow and to peak earlier compared to the C_6H_6 distributions. The corresponding kinetic energy distributions of molecules with a higher internal energy are thus shifted to a higher peak energy by about 0.5 eV. Previously, molecular dynamics simulations showed that the kinetic energies of the desorbed molecules are strongly correlated with their internal energies [15], leading to differences in the time distributions as we observed in our experiments. However, it remains unclear how such a small difference in internal energy (the vibrational state lies only 0.1 eV above the ground state) can lead to such vastly different time distributions. The populations in more states, preferably in different vibrational modes, should be probed to rule out the possibility that the differences in the time-distributions have a state-dependent origin.

At high coverages (Fig. 2b) the time distribution of the $C_6H_6^*$ is depleted from collisionally ejected molecules. A possible explanation for this observation is that in thick layers only the first few collisions between an escaping substrate atom and an adsorbate molecule are energetic enough to excite the molecule. Before this excited molecule can become detected, it has to travel through the thick molecular overlayer where intermolecular collisions are abundant. Collisional quenching or unimolecular decomposition are thus likely to occur. These experiments indicate that only $C_6H_6^*$ molecules created near the benzene-vacuum interface have a sufficiently high probability to survive de-excitation [9].

6. Ion-induced erosion of organic self-assembled monolayers

Self-assembled monolayers (SAMs) are ordered molecular assemblies that are spontaneously formed by the adsorption of an active surfactant on a solid surface. They have many promising applications in different technological fields such as nanofabrication, chemical and biological sensing, as well as tribology [1]. The most widely studied SAMs consist of a short hydrocarbon chains with functional groups at either end [19]. The molecules within the SAM are covalently bound to a substrate and the interchain interactions (e.g. van der Waals forces or dipole-dipole interactions) drive the formation of highly ordered and densely packed monolayers. We studied the erosion of SAMs made of phenethyl mercaptan $C_6H_5CH_2CH_2SH$

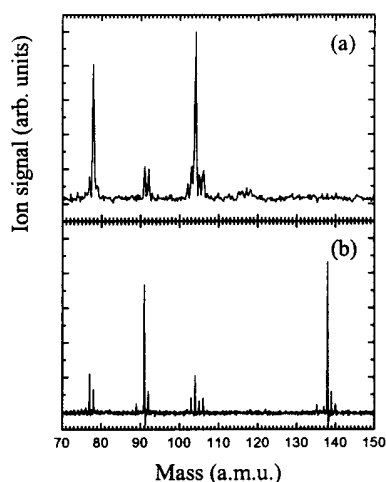


Fig. 3. Mass spectra of neutral molecules (a) emitted from 8 keV Ar^+ ion bombarded phenethyl mercaptan self-assembled monolayer and (b) photo-ionized gas-phase molecules.

(PEM) adsorbed to a gold substrate during bombardment with 8 keV Ar^+ ions [20-23].

The monolayers were prepared by submersing a vapor-deposited gold substrate in a 30 mM ethanol solution of these molecules for at least 24 hours prior to use. Next, the substrates were rinsed with ethanol before introduction into the analysis chamber to remove excess unbound molecules from the surface. Two-photon laser ionization was performed at 259.04 nm.

The mass spectrum of photo-ionized neutral molecules sputtered from

PEM/Au is shown in Fig. 3a, and compared with the mass spectrum obtained after photo-ionization of PEM molecules in the gas phase (Fig. 3b). The mass spectrum obtained in the sputtering experiment is dominated by the fragments at $m/z = 104$ and $m/z = 77$, which originate from the desulfurized PEM-molecule and the phenyl ring respectively. The complete PEM-molecule is hardly observable in this spectrum but ubiquitously present in the mass spectrum recorded during the gas phase experiment. From these observations it can be concluded that a substantial fraction of large fragments are emitted from the surface and are not solely the product of the photofragmentation of larger molecules.

A typical flight-time density distribution of laser post-ionized neutral molecular PEM fragments with $m/z = 104$ after ion-bombardment is shown in Fig. 4. The majority of the fragments reach the post-ionization region only after very long flight times (peak labeled "T" in the figure), indicating that those fragments predominantly desorb from PEM/Au with thermal energies. This is surprising since the PEM molecules are strongly bound to the gold substrate (the Au-S bond is about 2-3 eV) while the binding energy between the S and C atoms is of the same order [19]. Only a minor fraction of the emitted molecules has higher kinetic energies (peak "B" in the figure). A careful analysis using different projectiles showed that these molecules are

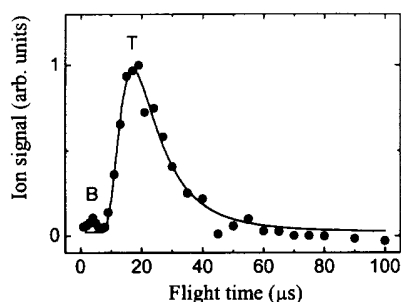
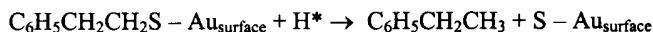


Fig. 4. Flight-time density distribution of the molecular fragment with $m/z = 106$ a.m.u. emitted from ion-bombarded PEM. The symbols represent the experimental data, taken at room temperature. The labels point to the peaks in the distribution caused by fast ("B") and slow ("T") fragments. The solid line indicates the best fit of the Maxwell-Boltzmann density distribution to the data.

sputtered with kinetic energies of the order of 1 eV by direct momentum transfer from the incident to the gold substrate and finally to the organic overlayer [23].

We postulated that the low-energy emission of PEM fragments can be explained by chemical reactions stimulated by the primary ions. Direct bond scission by projectile impact can be excluded since it would cause the molecules to be ejected with high kinetic energy. Molecular dynamics

simulations revealed that many of the surface molecules near the primary ion impact zone are severely damaged and yield reactive hydrogen-like species (protons, hydrogen-radicals ...) H^* as well as other ionic and neutral molecular fragments [15,24]. These unstable species can react with molecules and sever the chemical bonds. A possible reaction might be the following:



Bond scission by chemical reactions is more gentle than direct bond scission by ion impact and is more likely to form products which may be trapped at the surface until they finally are released with low kinetic energies. Direct scission of the Au-S bond is endothermic by approx. 2-3 eV, while cleavage by reaction with a hydrogen radical is estimated to be exothermic by 1.7 eV [23]. If evaporation is involved, the process should be temperature dependent. Indeed, such dependence has been observed and described by a convolution of the Maxwell-Boltzmann distribution with a first-order rate equation to account for the delay in the overall desorption [20,23].

The concepts presented here, are currently further under investigation using another class of thiol-based SAMs [22]. These molecules carry a biphenyl structure as a functional group, which is known to show an increased resistance to certain types of etching when irradiated with low-energy electrons, presumably because of electron-induced cross-linking between neighboring phenyl groups. Possibilities to use such molecules as ultrathin negative resists for electron lithography purposes are in an

exploratory phase [25,26]. A better understanding of the nature and an estimate of the fraction of desorbed fragments during particle-irradiation is thus highly desirable to improve the resolution that can be reached with this type of resist.

7. Summary

In conclusion, we demonstrated how laser ionization in combination with mass spectrometry is a versatile and extremely sensitive technique to study particle – solid interactions. The combined interpretation of the observables accessible with this technique, including population partitions, (quantum-state selective) velocity and angular distributions, and molecular fragmentation patterns, allows for gaining valuable insight in particle-induced desorption processes. These processes were found to depend strongly on the physical and chemical nature of the system under study.

We presented results from three case studies of systems with increasing chemical complexity subjected to a bombardment with keV Ar^+ ions. In the first case, the dominant contribution of resonant electron transfer in governing the final electronic configuration of metastable atoms emitted from clean metallic surfaces was presented. Next, the ejection of substrate atoms as well as intact molecules with different internal energies from ion-bombarded $\text{C}_6\text{H}_6/\text{Ag}(111)$ was found to be strongly coverage-dependent. Finally, we discussed how both ballistic processes as well as chemical reactions lead to the desorption of molecular fragments from highly ordered self-assembled monolayers covalently bound to a gold substrate.

In the future, we will continue studying the interactions of different projectiles with systems that are fundamentally as well as technologically relevant. Increasingly realistic and sophisticated molecular dynamics simulations will parallel these experimental studies. We are convinced that this is a powerful approach to derive conclusions not only on the dynamics of the ejection processes, but also on the reaction pathways taking place upon particle-irradiation.

Acknowledgements

This work is financially supported by the Fund for Scientific Research Flanders (F.W.O. - Vlaanderen), by the Flemish Concerted Action (G.O.A.) Research Program and by the Interuniversity Poles of Attraction (I.U.A.P.) Program - Belgian State, Prime Minister's Office - Federal Office for Scientific, Technical and Cultural Affairs. E.V is a Postdoctoral Fellows of the F.W.O. - Vlaanderen. Furthermore, the financial support of the National Science Foundation, the National Institutes of Health, the Office of Naval Research, and the Polish Committee for Scientific Research Fund are gratefully acknowledged.

References

- [1] A. Ulman (ed.), *Organic Thin Films and Surfaces – Directions for the Nineties* (Academic Press, San Diego, 1995).
- [2] P. Sigmund, in *Sputtering by particle bombardment I*, ed. R. Behrisch (Springer, Berlin, 1981) 9.
- [3] M.L. Yu, in *Sputtering by particle bombardment III*, eds. R. Behrisch, K. Wittmaack (Springer, Berlin, 1991) Chapter 3.
- [4] B.J. Garrison, N. Winograd, R. Chatterjee, Z. Postawa, A. Wucher, E. Vandeweert, P. Lievens, V. Philipsen, and R.E. Silverans, *Rap. Comm. in Mass Spectrom.* **12** (1998) 1266.
- [5] R. Chatterjee, D.E. Riederer, Z. Postawa, and N. Winograd, *Rap. Comm. in Mass Spectrom.* **12** (1998) 1226.
- [6] E. Vandeweert, V. Philipsen, W. Bouwen, P. Thoen, H. Weidele, R.E. Silverans, and P. Lievens, *Phys. Rev. Lett.* **78** (1997) 138.
- [7] E. Vandeweert, P. Lievens, V. Philipsen, J. Bastiaansen, and R.E. Silverans, *Phys. Rev. B*, in press (October 15th 2001).
- [8] P.H. Kobrin, G.A. Schick, J.P. Baxter, and N. Winograd, *Rev. Sci. Inst.* **57** (1986) 1354.
- [9] E. Vandeweert, C.A. Meserole, Z. Postawa, and N. Winograd, *Nucl. Instr. and Meth. in Phys. Res. B* **164-165** (2000) 820.
- [10] A. Wucher, M. Wahl, and H. Oechsner, *Nucl. Instr. and Meth. in Phys. Res. B* **82** (1993) 337.
- [11] P. Lievens, V. Philipsen, E. Vandeweert, and R.E. Silverans, *Nucl. Instrum. Meth. in Phys. Res. B* **135** (1998) 471.

- [12] E. Vandeweert, J. Bastiaansen, V. Philipsen, P. Lievens, and R.E. Silverans, Nucl. Instr. and Meth. in Phys. Res. B **164-165** (2000) 795; V. Philipsen, J. Bastiaansen, P. Lievens, E. Vandeweert, and R.E. Silverans, Vacuum **56** (2000) 269-274.
- [13] R.E. Silverans, J. Bastiaansen, V. Philipsen, E. Vandeweert, and P. Lievens, Nucl. Instr. and Meth. in Phys. Res. B **182** (2001) 127.
- [14] R. Chatterjee, D.E. Riederer, Z. Postawa, and N. Winograd, J. Phys. Chem. B. **102** (1998) 4176.
- [15] R. Chatterjee, Z. Postawa, N. Winograd, and B.J. Garrison, J. Phys. Chem. B **103** (1999) 151.
- [16] R. Dudde, K.H. Frank, and E.E. Koch, Surf. Sci. **225** (1990) 267.
- [17] C.A. Meserole, E. Vandeweert, Z. Postawa, Y. Dou, B.J. Garrison, and N. Winograd, Nucl. Instr. and Meth. in Phys. Res. B **180** (2001) 53-57.
- [18] J. H. Callomon, T.M. Dunn, and I.M. Mills, Phil. Trans. Roy. Proc. London **259A** (1966) 499.
- [19] A. Ulman, Chem. Rev. **96** (1996) 1533.
- [20] C.A. Meserole, E. Vandeweert, Z. Postawa, and N. Winograd, Applied Surface Science **141** (1999) 339.
- [21] P. Cyganik, Z. Postawa, C.A. Meserole, E. Vandeweert, and N. Winograd, Nucl. Instrum. and Meth. in Phys. Res. B **148** (1999) 137.
- [22] Z. Postawa, C. A. Meserole, P. Cyganik, J. Szymońska, and N. Winograd, Nucl. Instrum. and Meth. in Phys. Res. B **182** (2001) 148.
- [23] D.E. Riederer, R. Chatterjee, S.W. Rosencrance, Z. Postawa, T.D. Dunbar, D.L. Allara, and N. Winograd, J. Am. Chem. Soc. **119** (1997) 8089.
- [24] A. Delcorte, X. Vanden Eynde, P. Bertrand, J.C. Vickerman, B. J. Garrison, J. Phys. Chem. B **104** (2000) 2673.
- [25] W. Geyer, V. Stadler, W.Eck, M. Zharikov, A. Götzhäuser, M. Grunze, Appl. Phys. Lett. **75** (1999) 2401.
- [26] D. Rading, R. Kesting, and A. Benninghoven, J. Vac. Sci. Technol. A **18** (2000) 312.